Nr. 69
25. February 2020

universität innsbruck
Institut für Mathematik

Preprint-Series: Department of Mathematics - Applied Mathematics

The conical Radon transform with vertices on triple lines

M. Haltmeier, S. Moon

APPLIEDMATHEMATICS

Technikerstraße 13 - 6020 Innsbruck - Austria
Tel.: +43 512 507 53803 Fax: +43 512 507 53898
https://applied-math.uibk.ac.at

PREPRINT

The conical Radon transform with vertices on triple lines

Sunghwan Moon*

Department of Mathematics, Kyungpook National University,
Daegu 41566, Republic of Korea (sunghwan.moon@knu.ac.kr)

Markus Haltmeier

Department of Mathematics, University of Innsbruck, Technikerstrasse 13,
6020 Innsbruck, Austria (markus.haltmeier@uibk.ac.at)

arXiv:2002.10730v1 [math.NA] 25 Feb 2020

Abstract

We study the inversion of the conical Radon which integrates a function in three-dimensional space from integrals over circular cones. The conical Radon recently got significant attention due to its relevance in various imaging applications such as Compton camera imaging and single scattering optical tomography. The unrestricted conical Radon transform is over-determined because the manifold of all cones depends on six variables: the center position, the axis orientation and the opening angle of the cone. In this work, we consider a particular restricted transform using triple line sensor where integrals over a three-dimensional set of cones are collected, determined by a one-dimensional vertex set, a one-dimensional set of central axes, and the one-dimensional set of opening angle. As the main result in this paper we derive an analytic inversion formula for the restricted conical Radon transform. Along that way we define a certain ray transform adapted to the triple line sensor for which we establish an analytic inversion formula.

Keywords. Conical Radon transform, Compton camera, inversion, reconstruction formula.

AMS classification numbers. 44A12; 65R10; 92C55

*corresponding author

PREPRINT

1 Introduction

The conical Radon transform maps a function $f\colon \mathbb{R}^3 \to \mathbb{R}$ in three-dimensional space to its integrals over one-sided circular cones,

$$\mathbf{C}f(\mathbf{u},\boldsymbol{\beta},\psi) = \int_{\mathbb{S}^2}\int_0^\infty f(\mathbf{u}+r\boldsymbol{\alpha})r\delta(\boldsymbol{\alpha}\cdot\boldsymbol{\beta}-\cos\psi)\mathrm{d}r\mathrm{d}S(\boldsymbol{\alpha})$$

for $(\mathbf{u},\boldsymbol{\beta},\psi) \in \mathbb{R}^3\times\mathbb{S}^2\times[0,\pi]$. Here the cones of which the function is integrated are described by the vertex $\mathbf{u}\in\mathbb{R}^3$, the central axis $\boldsymbol{\beta}\in\mathbb{S}^2$ and the opening angle $\psi\in[0,\pi]$, and δ denotes the one-dimensional delta-distribution. Inverting the unrestricted conical Radon transform is over-determined as $\mathbf{C}f$ depends on six variables whereas the unknown function only depends on three. Various forms of conical Radon transforms arise by restricting to certain subsets of cones. Several inversion formulas for various types of conical transforms have derived in [4–6, 8–10, 12–17, 19, 20, 22, 23, 26]. Also, as a special two-dimensional version of the conical Radon transform, the V-line transform is also studied in [3, 11]. For a recent review of conical Radon transforms see [2, 18, 24]. In this paper we restrict the cones of integration to a three dimensional submanifold of conical surfaces associated to linear detector where vertices and the axes directions are restricted to one dimension.

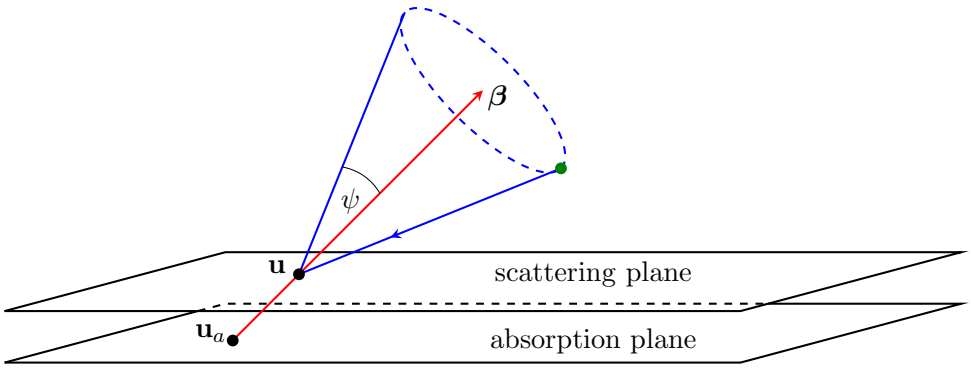

Figure 1: Schematic representation of a standard Compton camera

Among others, inverting the conical Radon transform is relevant for Compton camera imaging. A Compton camera (also called electronically collimated γ-camera) has been proposed in [21, 25] for single photon emission computed tomography (SPECT) offering increased efficiency compared to a conventional γ-camera. A standard Compton camera consists of two planar detectors: a scatter detector and an absorption detector, positioned one behind the other. A photon emitted from a radioactive source toward the camera undergoes Compton scattering in the scatter detector, and is absorbed in the absorption detector positioned behind (see Figure 1). In each detector plane, the positions $\mathbf{u}$, $\mathbf{u}_\mathrm{a}$ and the energy of the photon are measured. The energy difference determines the scattering angle ψ under which the photon path has been scattered at the scattering detector. Therefore, the measurements allow to conclude that photon has been emitted on a conical surface with vertex $\mathbf{u}$, axis direction

PREPRINT

pointing form $\mathbf{u}_a$ to $\mathbf{u}$ and opening angle ψ. In a similar manner, assuming a continuous source distribution of emitting photons, the Compton camera yields the conical Radon transform of source distribution with vertices restricted to the scattering plane. The corresponding data depend on five variables.

Instead of planar Compton cameras in this paper we consider linear Compton cameras consisting of two parallel detector lines (left image in Figure 2). Basically, the data acquisition with linear detectors is the same as in the standard one. The only difference is that the vertices are restricted to the one-dimensional scattering detector and the axes directions are restricted to the one-dimensional set of all directions pointing from the linear absorption detector to the linear scattering detector. Thus, the corresponding data depend on three variables and thus are no longer over-determined. As the main theoretical result of this paper, we derive an analytic inversion formula for triple linear sensor. As shown in the right image in Figure 2, the triple line sensor consists three one dimensional vertex sets Ξ_1, Ξ_2, Ξ_3 each associated with a one-dimensional set axis directions.

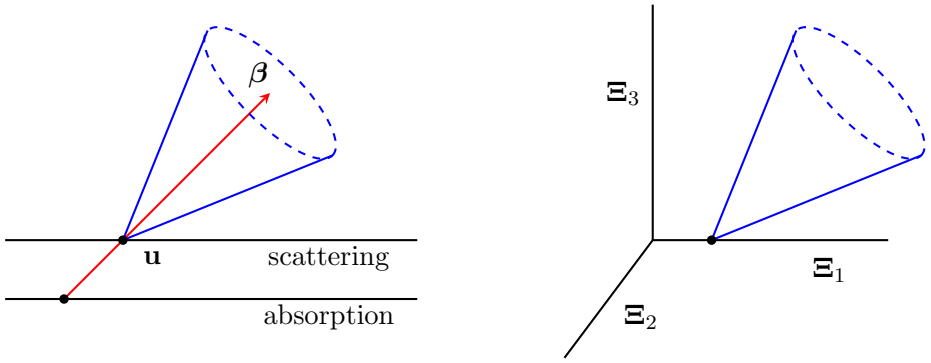

Figure 2: Left: Schematic representation of a Compton camera with line detectors. Right: Triple line detector consisting of three orthogonal lines.

In practice it may be easier to build linear detectors than planar detectors because the former requires less physical space and less complicated electronics. Moreover, to the high dimensionality of the data obtained from the planar detectors methods only using partial data have been derived (see e.g. [4–6, 10, 16, 19, 22]). On the other hand, Compton camera data are considerably noisy and utilizing full five-dimensional data is advised to obtain accurate reconstruction results [1, 7]. However, the data of planar sensors can be grouped in data sets of several virtual linear detectors. Therefore, inversion methods for line detectors can be applied to give several reconstructions for planar detectors that can be aggregated for noise reduction.

The rest of this paper is organized as follows. The conical Radon transform with triple linear detector in introduced in Section 2. In Section 3 we derive an analytic inversion formula. As main ingredient of the proof we reduce the conical Radon transform to a weighted ray transform and proof a novel inversion formula for this ray transform. The paper concludes with a short summary and outlook presented in Section 4.

PREPRINT

2 The conical Radon transform

In this section, we formally define the conical Radon transform with vertices on triple lines. Let

$$\boldsymbol{\Xi} = \boldsymbol{\Xi}_1 \cup \boldsymbol{\Xi}_2 \cup \boldsymbol{\Xi}_3 \tag{1}$$

be the set of vertices where

$$\begin{aligned} \boldsymbol{\Xi}_1 &\coloneqq \{(y_1, 0, 0) \colon y_1 \in [0,1]\} \\ \boldsymbol{\Xi}_2 &\coloneqq \{(0, y_2, 0) \colon y_2 \in [0,1]\} \\ \boldsymbol{\Xi}_3 &\coloneqq \{(0, 0, y_3) \colon y_3 \in [0,1]\}\,. \end{aligned} \tag{2}$$

We denote by $\psi \in [0, \pi]$ the opening angle of the circular cone and consider for each of the sets $\boldsymbol{\Xi}_j$ a different one-dimensional set of central axes. More precisely we parametrize each of the sets of central axes with $\bar{\boldsymbol{\beta}} = (\beta_1, \beta_2) \in \mathbb{S}^1$ and define

$$\boldsymbol{\beta}_{\mathbf{u}} = \begin{cases} (\beta_1, 0, \beta_2) & \text{if } \mathbf{u} \in \boldsymbol{\Xi}_1 \\ (0, \beta_1, \beta_2) & \text{if } \mathbf{u} \in \boldsymbol{\Xi}_2 \\ (\beta_1, 0, \beta_2) & \text{if } \mathbf{u} \in \boldsymbol{\Xi}_3\,. \end{cases} \tag{3}$$

Let $f \colon \mathbb{R}^3 \to \mathbb{R}$ be the distribution of the radioactivity sources.

For the following it is convenient to work with $s = \cos\psi \in [-1, 1]$. We then define the conical Radon transform $\mathbf{C}_k f$ of a function $f \in C(\mathbb{R}^3)$ with compact support as follows.

Definition 1 (Conical Radon transform)**.** *For given $k \in \mathbb{N}$ we define the conical Radon transform $\mathbf{C}_k f \colon \boldsymbol{\Xi} \times \mathbb{S}^1 \times \mathbb{R} \to \mathbb{R}$ with vertices on triple lines by*

$$\mathbf{C}_k f(\mathbf{u}, \bar{\boldsymbol{\beta}}, \psi) \coloneqq \begin{cases} \int_{\mathbb{S}^2} \int_0^\infty f(\mathbf{u} + r\boldsymbol{\alpha}) r^k \delta(\boldsymbol{\alpha} \cdot \boldsymbol{\beta}_{\mathbf{u}} - s)\, \mathrm{d}r\, \mathrm{d}S(\boldsymbol{\alpha}) & \text{if } s \in [-1, 1] \\ 0 & \text{otherwise}\,. \end{cases} \tag{4}$$

Here $\boldsymbol{\Xi}$ and $\boldsymbol{\beta}_{\mathbf{u}}$ are defined by (1)-(3)*, δ is the one-dimensional delta-distribution and* $\mathrm{d}S$ *is the standard area measure on the unit sphere $\mathbb{S}^2$,*

$$\mathrm{d}S(\boldsymbol{\alpha}) = \delta\Big(1 - \sqrt{\alpha_1^2 + \alpha_2^2 + \alpha_3^2}\Big)\mathrm{d}\alpha_1 \mathrm{d}\alpha_2 \mathrm{d}\alpha_3 \quad \text{for } \boldsymbol{\alpha} = (\alpha_1, \alpha_2, \alpha_3) \in \mathbb{R}^3\,.$$

Assuming that the density of photons decreases geometrically and proportional to the distance from the source to detectors, then the data measured by a Compton camera are given by the transform $\mathbf{C}_1 f$. When the density decreases at a different power of distance, we need different values of k, see [12].

3 Exact inversion formula

In this section we derive an explicit inversion formula for the conical Radon transform. Along that way we introduce a weighted ray transform, show how the conical Radon transform can

be reduced to the weighted ray transform and derive an explicit inversion formula for the weighted ray transform.

Definition 2 (Weighted ray transform)**.** *Let* $\boldsymbol{\Xi}$ *be defined by* (1) *and set* $\operatorname{conv}(\boldsymbol{\Xi}) \coloneqq \{\mathbf{x} \in [0,1]^3 \colon x_1 + x_2 + x_3 \leq 1\}$*. We define the weighted ray transform* $\mathbf{P}_k f \colon \boldsymbol{\Xi} \times \mathbb{R}^3 \to \mathbb{R}$ *of a continuous compactly supported function* $f \colon \mathbb{R}^3 \to \mathbb{R}$ *by*

$$\forall (\mathbf{u}, \mathbf{w}) \in \boldsymbol{\Xi} \times \mathbb{R}^3 \colon \quad \mathbf{P}_k f(\mathbf{u}, \mathbf{w}) \coloneqq \int_0^\infty f(\mathbf{u} + r\mathbf{w}) r^k \mathrm{d}r \,. \tag{5}$$

It is easy to check that $\mathbf{P}_k f$ is homogeneous of degree $-(k+1)$ in the variable of $\mathbf{w}$, i.e., $\mathbf{P}_k f(\mathbf{u}, \mathbf{w}) = |\mathbf{w}|^{-(k+1)} \mathbf{P}_k f(\mathbf{u}, \mathbf{w}/|\mathbf{w}|)$ for $\mathbf{w} \neq 0$.

Lemma 3 (Reduction of the conical Radon transform to the ray transform)**.** *For* $f \in C^\infty(\mathbb{R}^3)$ *with compact support in* $\operatorname{conv}(\boldsymbol{\Xi})$*, we have*

$$\forall (\mathbf{u}, \mathbf{w}) \in \boldsymbol{\Xi} \times \mathbb{R}^3 \colon \quad \mathbf{P}_k f(\mathbf{u}, \mathbf{w}) = \frac{w_{\mathbf{u}}}{4\pi |\mathbf{w}|^{k+2}} \int_{\mathbb{S}^1} H_s \partial_s (\mathbf{C}_k f) \left(\mathbf{u}, \bar{\boldsymbol{\beta}}, \bar{\boldsymbol{\beta}} \cdot \frac{\bar{\mathbf{w}}_{\mathbf{u}}}{|\mathbf{w}|} \right) \mathrm{d}S(\bar{\boldsymbol{\beta}}) \,. \tag{6}$$

Here $H_s f(s) = \frac{1}{\pi} \int_{\mathbb{R}} \frac{f(t)}{s-t} \mathrm{d}t$ *is the Hilbert transform and we have written*

$$\bar{\mathbf{w}}_{\mathbf{u}} \coloneqq \begin{cases} (w_1, w_3) \in \mathbb{R}^2 & \text{if } \mathbf{u} \in \boldsymbol{\Xi}_1 \\ (w_2, w_3) \in \mathbb{R}^2 & \text{if } \mathbf{u} \in \boldsymbol{\Xi}_2 \\ (w_1, w_3) \in \mathbb{R}^2 & \text{if } \mathbf{u} \in \boldsymbol{\Xi}_3 \end{cases}$$

and $w_{\mathbf{u}}$ *for the component of* $\mathbf{w}$ *missing in* $\bar{\mathbf{w}}_{\mathbf{u}}$*.*

We omit the proof here since it can be similarly proved as in that of Theorem 5 in [13] with some minor modification. For more details, we refer the readers to [13].

Now we are ready to obtain the inversion formula for $\mathbf{C}_k f$.

Theorem 4 (Inversion formula for the conical Radon transform)**.** *Define the constant* $c_k \coloneqq \frac{1}{2^2 (2\pi)^3 (k-1)!}$ *and let* $f \in C^\infty(\mathbb{R}^3)$ *have compact support in* $\operatorname{conv}(\boldsymbol{\Xi})$*. Then,*

$$f(\mathbf{x}) = c_k \Delta_{\mathbf{x}} \begin{cases} \displaystyle\int_{\mathbb{S}^2} \int_{\mathbf{n}^\perp \cap \mathbb{S}^2} \int_{-\infty}^{\alpha_1} \int_{\mathbb{S}^1} \frac{\alpha_2 (\alpha_1 - \omega)^{k-2}}{|(\omega, \alpha_2, \alpha_3)|^{k+2}} (\partial_{u_1}^{k-1} H_s \partial_s \mathbf{C}_k f) \left(\Lambda(\mathbf{x}, \mathbf{n}), \bar{\boldsymbol{\beta}}, \bar{\boldsymbol{\beta}} \cdot (\omega, \alpha_3) \right) \\ \qquad \times \mathrm{d}\omega \mathrm{d}S(\bar{\boldsymbol{\beta}}) \mathrm{d}S(\boldsymbol{\alpha}) \mathrm{d}S(\mathbf{n}) \qquad \text{if } \Lambda(\mathbf{x}, \mathbf{n}) \in \boldsymbol{\Xi}_1 \\ \displaystyle\int_{\mathbb{S}^2} \int_{\mathbf{n}^\perp \cap \mathbb{S}^2} \int_{-\infty}^{\alpha_2} \int_{\mathbb{S}^1} \frac{\alpha_1 (\alpha_2 - \omega)^{k-2}}{|(\omega, \alpha_2, \alpha_3)|^{k+2}} (\partial_{u_2}^{k-1} H_s \partial_s \mathbf{C}_k f) \left(\Lambda(\mathbf{x}, \mathbf{n}), \bar{\boldsymbol{\beta}}, \bar{\boldsymbol{\beta}} \cdot (\omega, \alpha_3) \right) \\ \qquad \times \mathrm{d}\omega \mathrm{d}S(\bar{\boldsymbol{\beta}}) \mathrm{d}S(\boldsymbol{\alpha}) \mathrm{d}S(\mathbf{n}) \qquad \text{if } \Lambda(\mathbf{x}, \mathbf{n}) \in \boldsymbol{\Xi}_2 \\ \displaystyle\int_{\mathbb{S}^2} \int_{\mathbf{n}^\perp \cap \mathbb{S}^2} \int_{-\infty}^{\alpha_3} \int_{\mathbb{S}^1} \frac{\alpha_2 (\alpha_3 - \omega)^{k-2}}{|(\alpha_1, \alpha_2, \omega)|^{k+2}} (\partial_{u_3}^{k-1} H_s \partial_s \mathbf{C}_k f) \left(\Lambda(\mathbf{x}, \mathbf{n}), \bar{\boldsymbol{\beta}}, \bar{\boldsymbol{\beta}} \cdot (\alpha_1, \omega) \right) \\ \qquad \times \mathrm{d}\omega \mathrm{d}S(\bar{\boldsymbol{\beta}}) \mathrm{d}S(\boldsymbol{\alpha}) \mathrm{d}S(\mathbf{n}) \qquad \text{if } \Lambda(\mathbf{x}, \mathbf{n}) \in \boldsymbol{\Xi}_3 \,, \end{cases} \tag{7}$$

PREPRINT

where $\Lambda(\mathbf{x},\mathbf{n})$ *is any point in* $\boldsymbol{\Xi}\cap\{\mathbf{y}\in\mathbb{R}^3\colon(\mathbf{x}-\mathbf{y})\cdot\mathbf{n}=0\}$.

Proof. Notice that by the chain rule, we have for $\mathbf{u}\in\boldsymbol{\Xi}_1$

$$\begin{aligned}(\partial_{w_1}^{k-1}\mathbf{P}_1 f)(\mathbf{u},\mathbf{w}) &= \int_0^\infty r\partial_{w_1}^{k-1} f(\mathbf{u}+r\mathbf{w})\mathrm{d}r\\ &= \int_0^\infty \partial_{u_1}^{k-1} f(\mathbf{u}+r\mathbf{w})r^k\mathrm{d}r = (\partial_{u_1}^{k-1}\mathbf{P}_k f)(\mathbf{u},\mathbf{w})\,.\end{aligned}$$

Similarly, we have $(\partial_{w_2}^{k-1}\mathbf{P}_1 f)(\mathbf{u},\mathbf{w}) = (\partial_{u_2}^{k-1}\mathbf{P}_k f)(\mathbf{u},\mathbf{w})$ for $\mathbf{u}\in\{0\}\times[0,1]\times\{0\}$ and $(\partial_{w_3}^{k-1}\mathbf{P}_1 f)(\mathbf{u},\mathbf{w}) = (\partial_{u_3}^{k-1}\mathbf{P}_k f)(\mathbf{u},\mathbf{w})$ for $\mathbf{u}\in\boldsymbol{\Xi}_3$. Together with Cauchy's formula for repeated integration we obtain

$$\mathbf{P}_1 f(\mathbf{u},\mathbf{w}) = \frac{1}{(k-1)!}\begin{cases}\displaystyle\int_{-\infty}^{w_1}(w_1-\omega)^{k-2}(\partial_{u_1}^{k-1}\mathbf{P}_k f)(\mathbf{u},\omega,w_2,w_3)\mathrm{d}\omega & \text{if } \mathbf{u}\in\boldsymbol{\Xi}_1\\ \displaystyle\int_{-\infty}^{w_2}(w_2-\omega)^{k-2}(\partial_{u_2}^{k-1}\mathbf{P}_k f)(\mathbf{u},w_1,\omega,w_3)\mathrm{d}\omega & \text{if } \mathbf{u}\in\boldsymbol{\Xi}_2\\ \displaystyle\int_{-\infty}^{w_3}(w_3-\omega)^{k-2}(\partial_{u_3}^{k-1}\mathbf{P}_k f)(\mathbf{u},w_1,w_2,\omega)\mathrm{d}\omega & \text{if } \mathbf{u}\in\boldsymbol{\Xi}_3\,.\end{cases}$$

Recall that Rf be the 3-dimensional regular Radon transform, i.e.,

$$Rf(\mathbf{n},s) = \int_{\{\mathbf{x}\cdot\mathbf{n}=s\}} f(\mathbf{x})\mathrm{d}\mathbf{x} \qquad \text{for} \quad (\mathbf{n},s)\in\mathbb{S}^2\times\mathbb{R}.$$

Then, using the polar coordinates, one can easily verify that

$$\begin{aligned}Rf(\mathbf{n},\mathbf{x}\cdot\mathbf{n}) &= \int_0^\infty\int_{\mathbf{n}^\perp\cap\mathbb{S}^2} f(\Lambda(\mathbf{x},\mathbf{n})+r\boldsymbol{\alpha})r\mathrm{d}S(\boldsymbol{\alpha})\mathrm{d}r = \int_{\mathbf{n}^\perp\cap\mathbb{S}^2}\mathbf{P}_1 f\left(\Lambda(\mathbf{x},\mathbf{n}),\boldsymbol{\alpha}\right)\mathrm{d}S(\boldsymbol{\alpha})\\ &= \frac{1}{(k-1)!}\begin{cases}\displaystyle\int_{\mathbf{n}^\perp\cap\mathbb{S}^2}\int_{-\infty}^{\alpha_1}(\alpha_1-\omega)^{k-2}(\partial_{u_1}^{k-1}\mathbf{P}_k f)(\Lambda(\mathbf{x},\mathbf{n}),\omega,\alpha_2,\alpha_3)\mathrm{d}\omega\mathrm{d}S(\boldsymbol{\alpha})\\ \qquad\text{if } \Lambda(\mathbf{x},\mathbf{n})\in\boldsymbol{\Xi}_1\\ \displaystyle\int_{\mathbf{n}^\perp\cap\mathbb{S}^2}\int_{-\infty}^{\alpha_2}(\alpha_2-\omega)^{k-2}(\partial_{u_2}^{k-1}\mathbf{P}_k f)(\Lambda(\mathbf{x},\mathbf{n}),\alpha_1,\omega,\alpha_3)\mathrm{d}\omega\mathrm{d}S(\boldsymbol{\alpha})\\ \qquad\text{if } \Lambda(\mathbf{x},\mathbf{n})\in\boldsymbol{\Xi}_2\\ \displaystyle\int_{\mathbf{n}^\perp\cap\mathbb{S}^2}\int_{-\infty}^{\alpha_3}(\alpha_3-\omega)^{k-2}(\partial_{u_3}^{k-1}\mathbf{P}_k f)(\Lambda(\mathbf{x},\mathbf{n}),\alpha_1,\alpha_2,\omega)\mathrm{d}\omega\mathrm{d}S(\boldsymbol{\alpha})\\ \qquad\text{if } \Lambda(\mathbf{x},\mathbf{n})\in\boldsymbol{\Xi}_3\,.\end{cases}\end{aligned} \tag{8}$$

We have the well-known inversion formula for Rf, i.e., for $\mathbf{x} \in \mathbb{R}^3$,

$$f(\mathbf{x}) = \frac{1}{8\pi^2}\Delta_{\mathbf{x}} \left(\int\limits_{\mathbb{S}^2} Rf(\mathbf{n}, \mathbf{x}\cdot\mathbf{n}) \mathrm{d}S(\mathbf{n}) \right). \tag{9}$$

This implies that the function $f(\mathbf{x})$ is determined by the integrals of Rf over the hyperplanes passing through the point $\mathbf{x}$. Plugging (8) into (9), we obtain the inversion formula for f in terms of $\mathbf{P}_1 f$ as

$$f(\mathbf{x}) = \frac{1}{8\pi^2(k-1)!}\Delta_{\mathbf{x}} \begin{cases} \displaystyle\int\limits_{\mathbb{S}^2}\int\limits_{\mathbf{n}^\perp\cap\mathbb{S}^2}\int\limits_{-\infty}^{\alpha_1} (\alpha_1-\omega)^{k-2}(\partial_{u_1}^{k-1}\mathbf{P}_k f)(\Lambda(\mathbf{x},\mathbf{n}),\omega,\alpha_2,\alpha_3)\mathrm{d}\omega\mathrm{d}S(\boldsymbol{\alpha})\mathrm{d}S(\mathbf{n}) \\ \qquad \text{if } \Lambda(\mathbf{x},\mathbf{n}) \in \boldsymbol{\Xi}_1 \\ \displaystyle\int\limits_{\mathbb{S}^2}\int\limits_{\mathbf{n}^\perp\cap\mathbb{S}^2}\int\limits_{-\infty}^{\alpha_2} (\alpha_2-\omega)^{k-2}(\partial_{u_2}^{k-1}\mathbf{P}_k f)(\Lambda(\mathbf{x},\mathbf{n}),\alpha_1,\omega,\alpha_3)\mathrm{d}\omega\mathrm{d}S(\boldsymbol{\alpha})\mathrm{d}S(\mathbf{n}) \\ \qquad \text{if } \Lambda(\mathbf{x},\mathbf{n}) \in \boldsymbol{\Xi}_2 \\ \displaystyle\int\limits_{\mathbb{S}^2}\int\limits_{\mathbf{n}^\perp\cap\mathbb{S}^2}\int\limits_{-\infty}^{\alpha_3} (\alpha_3-\omega)^{k-2}(\partial_{u_3}^{k-1}\mathbf{P}_k f)(\Lambda(\mathbf{x},\mathbf{n}),\alpha_1,\alpha_2,\omega)\mathrm{d}\omega\mathrm{d}S(\boldsymbol{\alpha})\mathrm{d}S(\mathbf{n}) \\ \qquad \text{if } \Lambda(\mathbf{x},\mathbf{n}) \in \boldsymbol{\Xi}_3\,. \end{cases} \tag{10}$$

Using Lemma 3, we have our assertion. □

Remark 5 (Generalization to different vertex sets)**.** *We point out that an inversion formula similar to* (7) *can also be derived for other arrangements triple line detectors. In such a case, one reconstructs a function $f \in C^\infty(\mathbb{R}^3)$ with compact support in a certain set K depending on $\boldsymbol{\Xi}$ by deriving generalizations of Lemma 3 and Theorem 4. For such results, the following condition has to be satisfied: For every $\mathbf{x} \in K$, every plane passing through $\mathbf{x}$ intersects the vertex set $\boldsymbol{\Xi}$.*

4 Conclusion

In this paper we derived an explicit inversion formula for inverting the conical Radon transform with vertices on triple lines. The considered geometry does not use formally over-determinated data and uses a bounded vertex set. As main auxiliary result we derived an inversion formula for a ray transform adjusted to the triple linear detector. While the used data was motivated by SPECT imaging with one-dimensional Compton cameras our results are applicable to other settings as well. In future work we will investigate then numerical implementation of the derived inversion approach and compare with other inversion methods.

PREPRINT

Acknowledgement

The work of S. M. was supported by the National Research Foundation of Korea grant funded by the Korea government (MSIP) (2018R1D1A3B07041149).

References

[1] M. Allmaras, D.P. Darrow, Y. Hristova, G. Kanschat, and P. Kuchment. Detecting small low emission radiating sources. *Inverse Problems and Imaging*, 7(1):47 – 79, 2013.

[2] G. Ambartsoumian. V-line and conical radon transforms with applications in imaging. *The Radon Transform: The First 100 Years and Beyond*, 22:143, 2019.

[3] G. Ambartsoumian and S. Moon. A series formula for inversion of the V-line Radon transform in a disc. *Computers & Mathematics with Applications*, 66(9):1567 – 1572, 2013.

[4] R. Basko, G.L. Zeng, and G.T. Gullberg. Application of spherical harmonics to image reconstruction for the Compton camera. *Physics in Medicine and Biology*, 43(4):887–894, 1998.

[5] J. Cebeiro, M. Morvidone, and M.K. Nguyen. Back-projection inversion of a conical Radon transform. *Inverse Problems in Science and Engineering*, 0(0):1–25, 0.

[6] M.J. Cree and P.J. Bones. Towards direct reconstruction from a gamma camera based on Compton scattering. *IEEE Transactions on Medical Imaging*, 13(2):398–409, 1994.

[7] Y. Feng, A. Etxebeste, D. Sarrut, J. M. Ltang, and V. Maxim. 3d reconstruction benchmark of a compton camera against a parallel hole gamma-camera on ideal data. *IEEE Transactions on Radiation and Plasma Medical Sciences*, page to appear, 2020.

[8] R. Gouia-Zarrad. Analytical reconstruction formula for n-dimensional conical Radon transform. *Computers & Mathematics with Applications*, 68(9):1016 – 1023, 2014.

[9] R. Gouia-Zarrad and G. Ambartsoumian. Exact inversion of the conical Radon transform with a fixed opening angle. *Inverse Problems*, 30(4):045007, 2014.

[10] M. Haltmeier. Exact reconstruction formulas for a Radon transform over cones. *Inverse Problems*, 30(3):035001, 2014.

[11] M. Haltmeier, S. Moon, and D. Schiefeneder. Inversion of the attenuated v-line transform with vertices on the circle. *IEEE Transactions on Computational Imaging*, 3(4):853–863, Dec 2017.

[12] C. Jung and S. Moon. Inversion formulas for cone transforms arising in application of Compton cameras. *Inverse Problems*, 31(1):015006, 2015.

PREPRINT

[13] C. Jung and S. Moon. Exact inversion of the cone transform arising in an application of a Compton camera consisting of line detectors. *SIAM Journal on Imaging Sciences*, 9(2):520–536, 2016.

[14] V. Maxim. Filtered backprojection reconstruction and redundancy in Compton camera imaging. *IEEE Transactions on Image Processing*, 23(1):332–341, 2013.

[15] V. Maxim, M. Frandeş, and R. Prost. Analytical inversion of the Compton transform using the full set of available projections. *Inverse Problems*, 25(9):095001, 2009.

[16] S. Moon. On the determination of a function from its conical Radon transform with a fixed central axis. *SIAM Journal on Mathematical Analysis*, 48(3):1833–1847, 2016.

[17] M. K Nguyen, T. T Truong, H. D Bui, and J. L Delarbre. A novel inverse problem in γ-rays emission imaging. *Inverse Problems in Science and Engineering*, 12(2):225–246, 2004.

[18] M K Nguyen and TT Truong. The development of radon transforms associated to compton scatter imaging concepts. 2018.

[19] M.K. Nguyen, T.T. Truong, and P. Grangeat. Radon transforms on a class of cones with fixed axis direction. *Journal of Physics A: Mathematical and General*, 38(37):8003–8015, 2005.

[20] D. Schiefeneder and M. Haltmeier. The radon transform over cones with vertices on the sphere and orthogonal axes. *SIAM Journal on Applied Mathematics*, 77(4):1335–1351, 2017.

[21] M. Singh. An electronically collimated gamma camera for single photon emission computed tomography. Part I: Theoretical considerations and design criteria. *Medical Physics*, 10(37):421–427, 1983.

[22] B. Smith. Reconstruction methods and completeness conditions for two Compton data models. *Journal of the Optical Society of America A*, 22(3):445–459, March 2005.

[23] F. Terzioglu. Some inversion formulas for the cone transform. *Inverse Problems*, 31(11):115010, 2015.

[24] F. Terzioglu, P. Kuchment, and L. Kunyansky. Compton camera imaging and the cone transform: a brief overview. *Inverse Problems*, 34(5):054002, apr 2018.

[25] R.W. Todd, J.M. Nightingale, and D.B. Everett. A proposed gamma camera. *Nature*, 251(6):132–134, 1974.

[26] T.T. Truong, M.K. Nguyen, and H. Zaidi. The mathematical foundation of 3D Compton scatter emission imaging. *International Journal of Biomedical Imaging*, May 2007.